Developing New Methods for Radiometric Enhancement Using High Resolution Satellite Imagery

Sharaf El Din, E.
Tanta University, Faculty of Engineering, Public Works Engineering Department, Gharbeya, Egypt
E-mail: essam.helmy@f-eng.tanta.edu.eg

Abstract
Environmental remote sensing applications depend on multitemporal data acquired from satellite imagery; however, the grey value change, associated with a corresponding feature, caused by non-surface components, such as atmospheric, brightness, and/or sensor geometry conditions, is a big challenge. Therefore, radiometric normalization is essential to minimize the grey value discrepancies in order to compare satellite images using the same colour component, and consequently to manipulate them for numerous environmental applications. By doing this, we guarantee that the grey value differences among temporal images can reflect real changes on the Earth's surface instead of representing false changes. In this research paper, relative radiometric normalization methods such as, histogram matching, simple regression, pseudo invariant features, dark and bright set, and no-change set, have been analyzed and tested using QuickBird images. Furthermore, pseudo invariant features and dark and bright set methods have been redeveloped in terms of refining the criterion of nominating the normalization targets as well as the normalization coefficients. The modified pseudo invariant features and dark and bright set methods revealed the highest accuracy, (i.e., the highest radiometric similarities among the normalized and reference images), using both visual inspection and statistical analysis.

1. Introduction

High resolution satellite imagery is a vital source of information required for numerous land use/land cover applications, such as change detection, image classification, mosaic production, shifting cultivation, and deformation assessment, etc. (Ban, 2016, Fujikia et al., 2016 and Santra et al., 2019). Geometric adjustment and radiometric normalization are the first two preprocessing steps that should be implemented to the images. These two operations can certainly affect the accuracy of the final product. Geometric registration transforms satellite images into the same geographic coordinate system. Similarly, radiometric normalization combines color data into a common color metric system. Without radiometric correction, it is very difficult to distinguish differences in multitemporal images under non-surface circumstances, such as illumination, atmospheric, or sensor characteristics (Chavez and Mackinnon, 1994).

Two main categories of radiometric enhancement can be performed: Absolute and Relative. Absolute radiometric normalization depends mainly on modeling the physical environment, such as atmospheric scattering, absorption, etc., at the same acquisition time (Shehhi et al., 2017). On the other hand, relative radiometric normalization can be implemented to images in order to eliminate radiometric differences by reason of non-surface elements (Hall et al., 1991 and Yang and Lo, 2000). Relative radiometric normalization is a correlation approach that utilizes one image as a reference and controls radiometric properties of the rest of images (i.e., subject images) to match the reference image (Yuan and Elvidge 1996 and Gorrono et al., 2017). Basically, relative radiometric normalization approach is superior because no physical information are required at the same time of satellite overpass because subject images can keep the same atmospheric errors as the reference image. Hence, all images appear to have been acquired under the same illumination and atmospheric conditions (Afify, 2002 and Du et al., 2002). There are some problems and limitations associated with image normalization. First, most published papers on image normalization were based on Landsat MSS, TM, or ETM data. Second, one of the relative radiometric normalization methods (i.e., no-change set (NC) method) requires two near-infrared wavelengths, while for QuickBird images, there is only one near-infrared band.

Third, other methods, such as pseudo invariant features (PIF) and dark and bright set (DB) need a new strategy to properly select the normalization targets and consequently the normalization coefficients (Hong and Zhang, 2007). Therefore, the purpose of this research paper is to find out methods that can be implemented to overcome the previous problems and limitations and can be effective in normalizing images. In this research paper, five methods have been carried out to radiometrically normalize the selected QuickBird images, which were captured in 2002 and 2007. The two images were acquired over the selected study area of Alexandria city, Egypt. The relative radiometric normalization methods are:

1. Histogram matching (HM).
2. Simple regression (SR).
3. Pseudo invariant features (PIF).
4. Dark and bright set (DB).
5. No-change set (NC).

In addition to the implementation of the previous relative radiometric normalization methods, in this research paper, some improvements have been presented to both PIF and DB. These improvements include a novel procedure for nominating the normalization targets, which can be then used for determining normalization coefficients for PIF and DB methods. After the implementation of the relative radiometric normalization methods, a set of multi-temporal normalized images have been produced and then visually and statistically compared to their counterparts of the reference image. Statistical analysis include determining the normalization coefficients, coefficient of variation (CV), dynamic range (DR), and the root mean square error (RMSE) for all bands to find out the proper method which can give the highest accuracy (i.e., the highest radiometric similarities among the normalized and reference images).

The identified objectives of this research are to (1) verify the potential of applying the existing relative radiometric normalization methods to high resolution QuickBird images and (2) develop two new methods: modified PIF (PIF-mod) and modified dark and bright set (DB-mod), and these methods generate normalized images that look very similar to their counterparts of the reference image (i.e., eliminating non-surface distortions). To the best of my knowledge, the modifications/improvements, which have been applied to both PIF and DB methods are developed for the first time to minimize the radiometric differences caused by non-surface components rather than changes in surface reflectance between the reference and subject images.

2. Material and Methods
2.1 Study Area
The study area represents a part of Alexandria city, Egypt, which lies among 28º 00' N and 32º 00' N, and 24º00' E and 30º 00' E. It shows intensive urban features, such as residential buildings, industrial entities, and extensive traffic network. Numerous industrial features reside in the lower right corner of the selected study area. The area is relatively flat with small elevation variation of about 20 m. As shown in Figure 1, the area of the study site is 1.728 km^2, which is equivalent to a QuickBird subscene of 600 * 500 pixels at 2.4 m ground resolution.

Figure 1: the selected study area

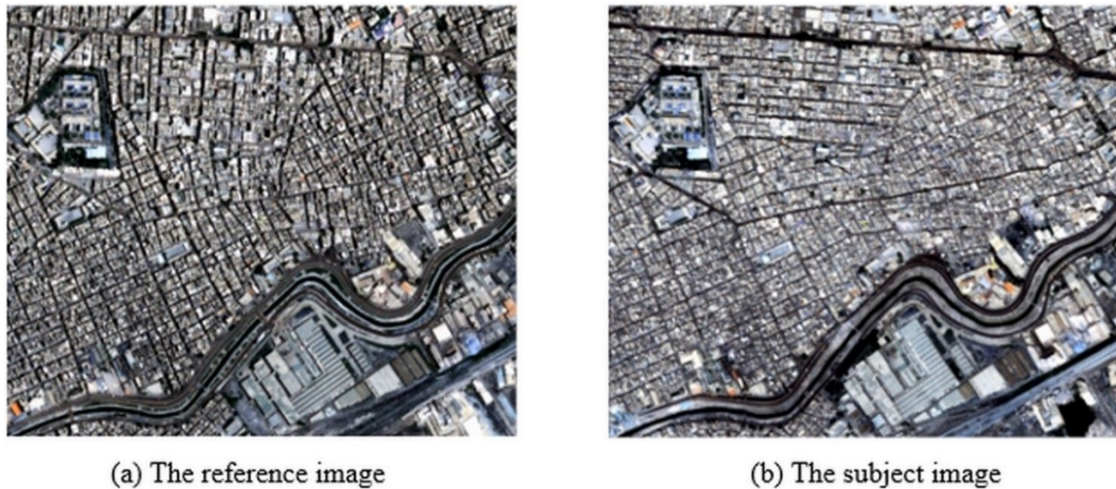(a) The reference image   (b) The subject image

Figure 2: the QuickBird reference and subject subscenes

Two QuickBird subscenes, which cover the study site were utilized in this research study. One image was nominated as a reference and the other was selected as a subject, as shown in Figure 2. The reference image was captured on May 2nd, 2002 and the subject image was captured on May 7th, 2007. The two subscenes are available in four multispectral bands (blue, green, red, and Near-Infrared). The subject subscene was registered to the reference subscene by using forty five ground control points, and the second order polynomial equation was used as the mathematical model in the image registration process. The obtained Root mean square errors (RMSEs) are less than 1 pixel in both X and Y directions. The nearest neighbour resampling method was used to resample the subject image in order to maintain the original spectral characteristic of the reference image.

2.2 Existing Relative Radiometric Normalization Methods

Geometric correction of multitemporal images is a very essential proprocessing step prior to applying image normalization methods. The QuickBird 2002 subscene was considered as the reference image; while, 2007 subscene was selected as the subject image. The reason of selecting 2002 subscene as a reference is that it contains more clear and sharp features/details. The 2007 subject image was registered to the 2002 reference image using forty-five ground control points and the second order polynomial equations were used as the mathematical model to perform the coordinate transformation among the corresponding images and the nearest-neighbor resampling technique was applied to resample the subject image in order to

preserve the original grey values of the subject image.

Relative radiometric normalization performs an image as a master and manipulates the radiometric characteristics of slave images in order to best correlate the master (Hall et al., 1991). Relative radiometric normalization methods are categorized as follows:

2.2.1 Histogram matching (HM)

It is a commonly used image normalization method, which is integrated in commercial image processing packages (Richards, 1986). The histogram of a subject image should be equalized to obtain a new histogram, which is then should be modified to match the histogram of a reference image by relating the cumulative density functions of both subject and refernce images to each other according to the following equation:

$$DN_n = (P_r)^{-1} [Ps (DN_s)]$$

Equation 1

Where:
DN_n = the digital number of a pixel in the normalized image.
$(P_r)^{-1}$ = the inverse cumulative density function of the reference image.
P_s = the cumulative density function of the subject image.
DN_s = the digital number of a pixel in the subject image.

HM is a useful technique that matches spectral data captured at various dates with slightly different sun elevation angles (Yang and Lo, 2000).

2.2.2 Simple regression (SR)

The concept of this method is that the whole image is utilized in a pixel by pixel manner using a linear equation, and there is no need to nominate normalization targets (Jenson, 1983).

$$Y_i = a_i X_i + b_i$$

Equation 2

Where:

a_i and b_i = the normalization coefficients at a specific multispectral band (i).

Y_i and X_i = the grey values of both reference and subject images at a specific multispectral band (i).

2.2.3 Pseudo invariant features (PIF)

This method depends mainly on nominating features/objects with nearly invariant reflectance, such as concrete, asphalt roads, and rooftops, between two acquisition dates (Yang and Lo, 2000, Zhou et al., 2016 and Hanzeyu et al., 2021). These features are considered not to cause any significant radiometric changes among different dates. The gray values differencies among these invariant features are linearly related in order to produce the normalization process (Syariz et al., 2019). The equation of selecting invariant features (PIF_{set}) for QuickBird Images is:

$$PIF_{set} = \{(band\ 4\ /\ band\ 3) < 1.1\ and,\ band\ 4 > 400\}$$

Equation 3

Once PIF_{set} is nominated in both reference and subject images, the normalization coefficients can be derived based on the selectes normalization targets (PIF_{set}) according to the following equations:

$$a_i = \sigma_{Yi} / \sigma_{Xi}$$

Equation 4

$$b_i = Y'_i - a_i X'_i$$

Equation 5

Where:

σ_{Yi} and σ_{Xi} = the standard deviation of PIF_{set} of both subject (Y) and reference (X) images at a specific multispectral band (i).

Y'_i and X'_i = the corresponding mean value of PIF_{set} of both subject (Y) and reference (X) images at a specific multispectral band (i).

2.2.4 Dark and bright set (DB)

This method assumes that each scene contains some pixels that have the same reflectance values between images acquired at different dates (Hall et al., 1991). For QuickBird images, the brightness-greenness transformation equations have been used as follows (Yarbrough et al., 2005):

Brightness = 0.319 (band1) + 0.542 (band2) + 0.490 (band3) + 0.604 (band4)

Equation 6

Greenness = -0.121 (band1) - 0.331 (band2) - 0.517 (band3) + 0.780 (band4)

Equation 7

After that, the formulas below have been applied to nominate the DB_{set} from QuickBird reference and subject images (Afify, 2011).

$$bright\ set = \{greenness \leq t_1\ and,\ brightness \geq t_2\}$$

Equation 8

$$dark\ set = \{greenness \leq t_1\ and,\ brightness \leq t_2\}$$

Equation 9

Where:

t_1 and t_2 = the threshold values for QuickBird images. The value t_1 is set to 1.00 and t_2 is set to 950 for bright set, while for dark set t_1 is set to 1.00 and t_2 is set to 460. Once both bright and dark sets have been calculated for refernce and subject images, the normalization coefficients can be determined according to the following equations:

$$a_i = (Y'^{(b)}_i - Y'^{(d)}_i) / (X'^{(b)}_i - X'^{(d)}_i)$$

Eqaution 10

$$b_i = Y'^{(d)}_i - a_i X'^{(d)}_i$$

Eqaution 11

Where:

$Y'^{(b)}_i$ and $Y'^{(d)}_i$ = the mean value of the bright set (b) of reference image (Y) and the mean value of the dark set (d) of reference image (Y) at a specific multispectral band (i).

$X'^{(b)}_i$ and $X'^{(d)}_i$ = the mean value of the bright set (b) of subject image (X) and the mean value of the dark set (d) of subject image (X) at a specific spectral band (i).

2.2.5 No-change set (NC)

This method constructs a linear scatterplot between the two nearinfrared wavelengths of both the reference and the subject images (Yuan and Elvidge, 1996). At the nearinfrared bands, spectral radiation of black pixels, such as water bodies is low, while spectral radiation of land pixels, such as concrete, asphalt, and rooftops is relatively high. Therefore, the spectral cluster centers for both land and water are clearly separated. After obtaining the coordinates of the two centers of land and water, a linear relationship can be developed between the reference and subject images, and therefore, the normalization coefficients are obtained. The NC normalization targets have been defined by the following equations:

$$NC_{set} = \{(Y_4 - a_{4o}X_4 - b_{4o}) \leq HVW\}$$

Equation 12

$$HVW = \sqrt{(1 + a_{40}{}^2)} * (HPW)$$

Eqaution 13

Where:

a_{4o} and b_{4o} = the initial normalization coefficients of the nearinfrared band.
HVW= the half vertical width of no change regions.
HPW = the half perpendicular width of no change regions.
Y_4 = the digital numbers of nearinfrared band of reference image Y.
X_4 = the digital numbers of nearinfrared band of subject image X.

Once the no-change pixels are found, they are used for deriving the final normalization coefficients for each band. This can be derived by applying a least square regression method.

2.2.6 (New method 1) Modified Pseudo invariant features (PIF_mod)

The author uses the logical operation "AND" to determine the modified PIF_{set} by using the intersection of the two individual PIF masks on both the refernce and subject images. Moreover, another improvement/modification is applied to derive the normalization coefficients from the modified PIFset by using a linear transformation that was figured out by a least squares technique. After that, the obtained normalization coefficients can be utilized to normalize the bands of the subject image and the difference bands are developed by subtracting the normalized bands from their corresponding reference bands and the root mean square errors (RMSEs) of the normalized images are determined.

2.2.7 (New method 2) Modified dark and bright set (DB_mod)

The author uses the logical operation "AND" to determine the modified DB_{set}, which contains the same pixels in both the refernce and subject images. Another improvement/modification involves the use of a linear transformation between the reference and subject images that is based mainly only on the modified DB_{set}. The modified DB_{set} is determined by grouping the modified dark set and the modified bright set using the logical operation "OR". Once the normalization coefficients are calculated, they are utilized to normalize the bands of the subject image. Then, the difference bands are produced by subtracting the normalized bands from their corresponding bands of the reference image, and therefore, the RMSEs of the normalized images can be calculated.

3. Results and Discussion

3.1 Statistical Differences between Relative Radiometric Normalization Methods

The results of various relative radiometric normalization methods were analyzed and then compared, visually and statistically, to each other and to the reference image as well. In terms of statistical analysis, coefficient of variation (CV), dynamic range (DR), root mean square error (RMSE), and normalization coefficients were calculated.

Coefficient of variation (CV) is measured by calculating the ratio of the standard deviation value to the mean value for a certain band; while, dynamic range (DR) is calculated by subtracting the minimum digital number from the maximum digital number for each band. For all the difference images, resulted from subtracting the normalized image from the reference image, the coefficient of variation (CV) and the dynamic range (DR) were determined and populated in Table 1. It is obvious that the lower CV and DR values, the more accurate normalized images can be obtained and consequently the normalized images can yield high matching to the reference image.

For all the normalized images, the CV and DR values are generally less than those of the raw image. This means that all the applied relative radiometric normalization methods have improved the radiometric similarity of the subject image to the reference image but with different degrees of improvement. Regarding the accuracy of the resulted normalized image, methods used in this study can be ranked in a descending order according to the resulted values of CV and DR of difference image as follows: DB-mod, PIF-mod, SR, NC, HM, DB, and PIF.For the selected relative radiometric

normalization methods, Table 2 shows the normalization coefficients gain (a) and offset (b) derived and applied for the subject image in a band by band manner in order to obtain the normalized image. For DB-mod, PIF-mod, SR, and NC methods, the gain value (a) is far from 1.00 (a = 0.32, 0.36, 0.39, and 0.56 for blue band, respectively) and the offset value (b) is away from zero (b = 293.58, 268.50, 218.36, and 149.64 for blue band, respectively). This ensures the effectiveness of the used normalization coefficients applied to normalize the subject image in a band by band manner resulting in the normalized images that appear radiometrically more similar to the reference image.

For DB and PIF methods, the gain value (a) is close to 1.00 (a = 0.83 and 0.99 for blue band, respectively) and the offset value (b) is near to zero (b = 38.71 and -53.79 for blue band, respectively). This means that the normalization coefficients introduced and applied for the subject image to match the reference are slightly efficient and the normalized images resulted from the previous methods yield poor matching to the reference image. As shown in Table 3, the RMSEs for all QuickBird raw bands are 90.78, 189.34, 175.69, and 187.52, respectively. On the other side, all of the normalized images led to less RMSEs compared to the raw data. As shown in

Table 1: coefficient of variation (CV) (multiplied by 100) and dynamic range (DR) for the selected methods

Method	Band 1		Band 2		Band 3		Band 4	
	C.V	D.R	C.V	D.R	C.V	D.R	C.V	D.R
RAW	19.40	1386	25.60	2286	31.51	2085	30.55	2205
HM	12.95	687	15.53	910	17.71	968	16.07	991
SR	7.33	381	9.51	596	11.55	622	10.99	698
PIF	18.12	997	23.24	1550	28.28	1650	26.47	1811
DB	14.67	834	18.56	1298	22.15	1370	21.08	1545
NC	10.34	560	13.16	865	15.47	888	13.81	932
PIF-mod	6.31	359	7.96	552	9.70	592	8.72	598
DB-mod	5.53	320	6.84	492	8.24	530	7.55	549

Table 2: normalization coefficients for the selected relative radiometric normalization methods at different bands

Method	Band(1)		Band(2)		Band(3)		Band(4)	
	a	b	a	b	a	b	a	b
HM	-	-	-	-	-	-	-	-
SR	0.39	218.36	0.40	330.44	0.40	245.91	0.42	261.93
PIF	0.99	-53.79	1.04	-109.72	1.06	-102.28	1.09	-123.36
DB	0.83	38.71	0.87	49.69	0.88	34.6	0.93	19.18
NC	0.56	149.64	0.58	225.90	0.57	176.62	0.56	205.06
PIF-mod	0.36	268.50	0.37	419.73	0.38	320.79	0.36	342.17
DB-mod	0.32	293.58	0.33	476.06	0.34	372.98	0.33	395.07

Table 3: number of pixels and RMSEs for all bands using the selected relative radiometric normalization methods

Method	No. of pixels (subject image)		No. of pixels (reference image)		R.M.S.E				
	Number	%	Number	%	Band 1	Band 2	Band 3	Band 4	Average
RAW	300000	100	300000	100	90.78	189.34	175.69	187.52	160.83
HM	300000	100	300000	100	77.12	158.89	147.46	159.81	135.82
SR	300000	100	300000	100	74.06	152.99	142.00	152.72	130.44
PIF	218725	72.91	163579	54.53	88.62	182.30	169.72	178.18	154.70
DB	1900 (D) 250429 (B)		952 (D) 169217 (B)						
	252329 (T)	84.11	170169 (T)	56.72	82.77	170.56	158.36	168.52	145.05
NC	22949	7.65	22949	7.65	76.02	156.78	145.14	154.49	133.10
PIF-mod	142117	47.37	142117	47.37	73.99	152.76	141.85	152.71	130.32
DB-mod	793 (D) 156491 (B)		793 (D) 156491 (B)						
	157284 (T)	52.43	157284 (T)	52.43	73.91	152.61	141.67	152.71	130.22

Figure 3, new developed methods (i.e., DB-mod and PIF-mod) gave better performance, (i.e, the normalized images are very close to the reference image in terms of radiometric similarities), followed by SR, NC, HM, DB, and PIF. That means the development/modifications introduced to refine the normalization targets and consequently to derive the normalization coefficients for PIF-mod and DB-mod methods have been found to be very efficient, since the radiometric similarities between the normalized images and their counterparts of the reference image have been improved.

As shown in Table 3, the accuracy of the normalized image obtained using NC method (i.e., RMSE = 133.10) is slightly lower than that obtained using SR method (i.e., RMSE = 130.44). However, the number of pixels used to derive the normalization coefficients in NC method is about 8% of the number of pixels used in SR method. This proves the capability of NC method to select a very few image samples that can represent the actual radiometric properties of the whole image.

Moreover, as shown in Table 3, the RMSEs of the PIF-mod and DB-mod methods are very close to that obtained using the SR method; however, the number of pixels used to derive the normalization coefficients using PIF-mod and DB-mod methods is about 50% lower than the number of pixels used in SR method. Furthermore, using the normalization targets as the intersection between the two individual normalization targets assigned individually on both the reference and subject images have improved the accuracy of DB method about 10% (the RMSE decreased from 145.05 for

DB method to 130.22 for DB-mod method) and also improved the accuracy of PIF method by about 16% (the RMSE decreased from 154.70 for PIF method to 130.32 for PIF-mod method). The PIF-mod and DB-mod methods have showed higher accuracy compared to the typical methods because they depend mainly on selecting the normalization targets, which can represent features with nearly invariant reflection in the reference and subject images. This confirms the capability of the used refinement procedure to nominate the normalization targets, which are then used to derive the normalization coefficients resulting in the normalized images.

3.2 Visual Analysis of the Selected Relative Radiometric Normalization Methods

After the implementation of numerous RRN methods, the result is a collection of multi-temporal bands that appear to have been acquired under the same illumination, atmospheric and sensor geometry conditions with their corresponding reference bands. The original QuickBird images and the normalized images are shown in Figure 4. Visually, from Figure 4, it can be noted that the DB-mod, PIF-mod, SR, and NC methods look very similar, and therefore, it is difficult to determine which one of these normalized images is the best. Methods generated using no change pixels, such as DB-mod, PIF-mod, and NC methods, tend to reduce the false radiometric differences caused by non-surface influences between the subject image and the reference image.

(a) the reference image

(b) the subject image

(c) HM normalized image

(d) SR normalized image

(e) PIF normalized image

(f) DB normalized image

Figure 3: The QuickBird reference, subject, and normalized subscenes (Continue next page)
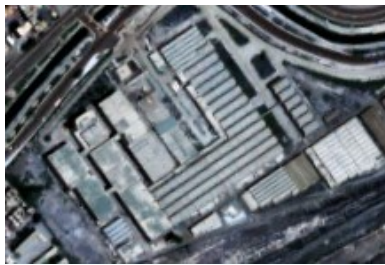
(g) NC normalized image

(h) PIF-mod normalized image

(i) DB-mod normalized image

Figure 3: the QuickBird reference, subject, and normalized subscenes

(a) the reference subscene

(b) HM normalized subscene

(c) SR normalized subscene

(d) PIF normalized subscene

Figure 4: the QuickBird reference and normalized subscenes

(e) DB normalized subscene

(f) NC normalized subscene

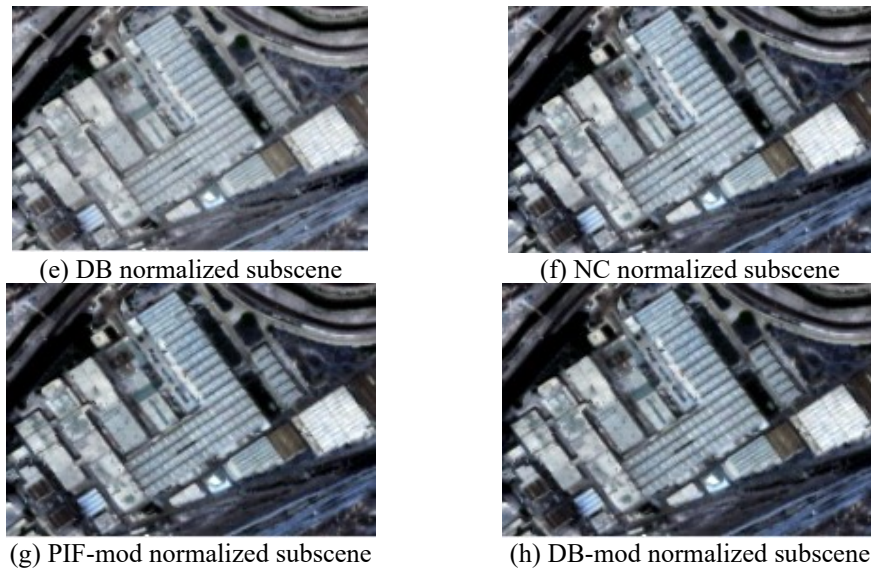(g) PIF-mod normalized subscene

(h) DB-mod normalized subscene

Figure 4: The QuickBird reference and normalized subscenes

Since the normalized images using these methods look very close to the reference image. For the DB-mod, PIF-mod, SR, and NC methods, different urban areas, factories, and industrial features, which are found in the lower right corner of the study area look similar to their counterparts of the reference image than the subject image, as shown in Figure 4. As shown in Figure 4, the DB, PIF, and HM methods are found to be dissimilar to the reference image. The features appear with the same color but different tones, especially for urban areas and industrial features, which are found in the lower right corner of the study area.

4. Conclusion
This study investigated the implementation of relative radiometric normalization methods for multi-temporal high resolution satellite images. In addition to developing two new methods, commonly used relative radiometric normalization methods have been carried out to radiometrically normalize multi-date QuickBird images. Enhancement/modifications regarding the nomination of normalization targets and the formula used to determine the normalization coefficients have been introduced to PIF set method and DB set method, and then examined to normalize the same multi-date images. The accuracy of the normalized images have been evaluated and tested both visually and statistically. After the implementation of the selected methods and analyzing the results, the following conclusions can be drawn:

1. Among all the selected methods, DB-mod method has provided the superior accuracy. It was followed by PIF-mod method with a very slightly lower accuracy. This confirms the suitability of the modifications suggested for selecting the normalization targets and for deriving the normalization coefficients.

2. The DB-mod and PIF-mod methods have produced normalized images with higher accuracy (less RMSE) than those obtained using the typical DB and PIF methods; however, the number of the normalization targets used for DB-mod and PIF-mod methods are much smaller than those used for typical DB and PIF methods. This demonstrates the effectiveness of the refinement procedure used to select less normalization targets, which can provide a comprehensive representation of the radiometric differences caused by non-surface subtleties rather than changes in surface reflectance.

3. The accuracy of the normalized image obtained by using NC set method is very close to that obtained using DB-mod, PIF-mod, and SR methods. The whole image pixels have been used to derive the normalization coefficients for SR method; however, DB-mod, PIF-mod, and NC methods have only utilized 50%, 50%, and 8%, respectively, of image pixels. Therefore, selecting the appropriate number of pixels that can represent a good selection of normalization targets is essential to minimize radiometric differences among multi-temporal images.

4. Methods that use all pixels in the subject and reference images to generate statistics, such as SR and HM, often work well if there are no big radiometric changes among multi-temporal images. However, other methods, such as NC set, PIF-mod, and DB-mod, that can employ small number of image pixels (i.e., normalization targets) perform very well, especially, in case of large radiometric changes between multi-temporal data are found.

5. Further implementation of previous methods including the modified methods over different regions should be considered in the future for further verification of the robustness of these methods.

Acknowledgements

References

Afify, H. A., 2002, Radiometric Normalization of Remotely Sensed Images: A New Approach Using Linear Scattergram Regression. *Alexandria Engineering Journal.* Vol. 41, No. 6, 1033-1040.

Afify, H. A., 2011, Improved Techniques for Relative Radiometric Normalization of QuikBird Multi-Temporal Images. *International journal of Geoinformatics.* Vol. 7(4), 1-11.

Ban, Y., 2016, *Multitemporal Remote Sensing: Methods and Applications.* Springer-Verlag, Berlin Heidelberg.

Chavez, P. S. and Mackinnon, D. J., 1994, Automatic Detection of Vegetation Changes in the Southwestern United States Using Remotely Sensed Images. *Photogrammetric Engineering and Remote Sensing*, Vol. 60, 571–583.

Du, Y., Teillet, P. M. and Cihlar, J., 2002, Radiometric Normalization of Multitemporal High Resolution Satellite Images with Quality Control for Land Cover Change Detection. *Remote Sens. Environ.*, Vol. 82, 123–134.

Fujikia, S., Okada, K., Nishio, S. and Kitayama, K., 2016, Estimation of the Stand Ages of Tropical Secondary Forests After Shifting Cultivation Based on the Combination of WorldView-2 and Time-Series Landsat Images. *ISPRS J. Photogramm. Remote Sens.*, Vol. 119, 280–293.

Gorrono, J., Banks, A. C., Fox, N. P. and Underwood, C., 2017, Radiometric Inter-Sensor Crosscalibration Uncertainty Using a Traceable High Accuracy Reference Hyperspectral Imagery. *ISPRS J. Photogramm. Remote Sens.* Vol. 130, 393-417.

Hall, F. G., Strebel, D. E., Nickeson, J. E. and Goetz, S. J., 1991, Radiometric Rectification. Toward a Common Radiometric Response among Multidate, Multisensor Images. *Remote Sensing of Environment*, Vol. 35, 11–27.

Hanzeyu, X., Yuchun, W., Xiao, L., Yadi, Z. and Qi, C., 2021, A Novel Automatic Method on Pseudo-Invariant Features Extraction for Enhancing the Relative Radiometric Normalization of High-Resolution Images. *International Journal of Remote Sensing*, Vol. 42(16), 6153-6183, DOI: 10.1080/01431-161.2021.1934912.

Hong G. and Zhang, Y., 2007, A Comparative Study on Radiometric Normalization Using High Resolution Satellite Images. *International Journal of Remote Sensing*, Vol. 29(2), 425-438.

Jenson, J. R., 1983, Urban/Suburban Land Use Analysis, In R.N. Colwell (Ed.), Manual of Remote Sensing, 2nd Ed.. American Society of Photogrammetry, Fall Church, VA, 1571-1666.

Richards, J. A., 1986, *Remote Sensing Digital Image Analysis: An Introduction.* Springer-Verlag, Berlin Heidelberg, XIX, 494, DOI: 10.1007/978-3-642-30062-2.

Santra, A., Mitra, S. S., Mitra, D. and Sarkar, A., 2019, Relative Radiometric Normalization - Performance Testing of Selected Techniques and Impact Analysis on Vegetation and Water Bodies. Geocarto International, Vol. 34(1), 98–113.

Shehhi, M. R., Gherboudj, I., Zhao, J. and Ghedira, H., 2017, Improved Atmospheric Correction and Chlorophyll-A Remote Sensing Models for Turbid Waters in a Dusty Environment. *ISPRS J. Photogramm. Remote Sens.*, Vol. 133, 46–60.

Syariz, M. A., Lin, B., Denaro, L. G., Jaelani, L. M., Nguyen, M. V. and Lin, C., 2019, Spectral-Consistent Relative Radiometric Normalization for Multitemporal Landsat 8 Imagery. *ISPRS Journal of Photogrammetry and Remote Sensing*, Vol. 147, 56-64.

Yang, X. J. and Lo, C. P., 2000, Relative Radiometric Normalization Performance for Change Detection from Multi-Date Satellite Images. *Photogrammetric Engineering and Remote Sensing*, Vol. 66, 967–980.

Yarbrough, L. D., Easson, G. and Kuszmaul, J. S., 2005, QuickBird 2 Tasseled Cap Transform Coefficients: A Comparison Of Derivation

Methods. *Proceeding of ASPRS Conference Pecora 16, October 23-27*, 2005, Sioux Falls, South Dakota.

Yuan, D. and Elvidge, C. D., 1996, Comparison of Relative Radiometric Normalization Techniques. *ISPRS Journal of Photogrammetry and Remote Sensing*, Vol. 51, 117–126.

Zhou, H., Liu, S., Jianjun, H., Wen, Q., Song, L. and Yanfei, M., 2016, A New Model for the Automatic Relative Radiometric Normalization of Multiple Images with Pseudo-invariant Features. *International Journal of Remote Sensing*, Vol. 37 (19), 4554–4573.